

# Spectrally selective 3D imaging of phosphocreatine in the human calf muscle at 3T and 7T

Prodromos Parasoglou<sup>1</sup>, Ding Xia<sup>1</sup>, Gregory Chang<sup>1</sup>, and Ravinder R Regatte<sup>1</sup>  
<sup>1</sup>Center of Biomedical Imaging, NYU Langone Medical Center, New York, New York, United States

**Introduction:** Imaging of a single <sup>31</sup>P metabolite (i.e phosphocreatine (PCr)) has shown great potential for studying the bioenergetics of skeletal muscle [1] offering much higher spatial and temporal resolution [2] compared to more traditional chemical shift imaging (CSI) methods. Most of the <sup>31</sup>P metabolites (including PCr) have long T<sub>1</sub> and T<sub>2</sub> values favoring the use of rapid spin-echo acquisition (turbo spin echo - TSE) techniques. In this work, we quantitatively compare the benefits and challenges of high-resolution spectrally selective 3D-imaging of PCr in the human calf muscle at 3T and 7T.

**Methods and Materials:** All the experiments were performed on 3T and 7T Siemens scanners (using two geometrically identical dual-tuned (<sup>31</sup>P/<sup>1</sup>H) quadrature volume coils (Rapid MRI, Ohio). Images were acquired through a fully centric 3D TSE, developed using the 'SequenceTree' software [3], a schematic of which is shown in Fig.1.a. The phase encode gradient waveform is shown in Fig.1.b. TSE parameters used: echo train length (ETL) 24;

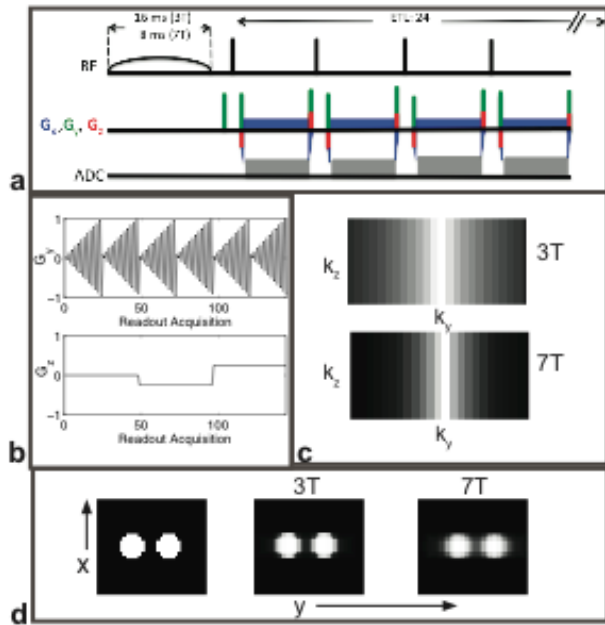


Fig. 1. **a**) Schematic of the developed TSE sequence. A spectral selective Gaussian RF pulse is employed followed by a train of non-selective refocusing pulses. The phase encode gradient in y direction (green) is applied simultaneously with the crusher gradients around the refocusing pulse. **b**) Phase encode gradient waveform in the y (top) and z (bottom) direction during six echo trains. **c**) Simulated MTF of the sampling pattern at 3T and 7T. **d**) Simulated blurring effect of the sampling pattern on a phantom at 3T and 7T.

with 25 mM and 50 mM, and Pi with 25 mM and 50 mM) for quantification of the metabolites in the muscle. Anatomical images were also acquired using a standard 3D-GRE sequence for <sup>1</sup>H with resolution of 1.7 x 1.7 x 5 mm and the same FOV and orientation as in the <sup>31</sup>P image. All the experiments were acquired on five healthy volunteers (3 male, 2 female, age 29-39 years).

**Results and Discussion:** In <sup>31</sup>P relaxation both dipolar relaxation and chemical shift anisotropy are major competing mechanisms [5] that lead to a decrease in T<sub>1</sub> at increased fields (PCr from 5.57±0.26 s at 3T to 3.53 ±0.18 s at 7T). T<sub>2</sub> relaxation times reduce at higher field (from 365±38 ms at 3T to 153±55 ms at 7T). An example of the measurement and fitting for one volunteer is shown in Fig.2.a,b. In TSE methods the echo amplitude is modulated as a function of the echo position in k-space, resulting in blurring and ghosting artifacts. This problem becomes more severe for shorter T<sub>2</sub> values. The modulation transfer function (MTF) has been simulated and shown in Fig.1.c by using the measured T<sub>2</sub> values at 3T and 7T respectively. The point spread function (PSF) was estimated based on the full-width-at-half-maximum (FWHM) of the Fourier transform of the MTF (1.6 pixels at 3T, and 2.8 pixels at 7T). Fig.1.c shows the increased blurring effect at 7T versus 3T. This effect can be reduced by shortening the echo spacing at 7T (PSF at 7T would be equal that of 3T for 13 ms echo spacing). However, there is a 2.8 fold increase in SNR at 7T as shown in Figure.3.a-b. Even in the case of the higher resolution image (half the voxel size) the SNR remains higher than in the 3T case.

**Conclusion:** Spectrally selective imaging of PCr in the human calf at 7T showed a 2.8 fold increase in SNR compared to that obtained at 3T. The increased blurring, due to shorter T<sub>2</sub> at 7T, can be compensated by reducing the echo-spacing at the expense of some SNR loss due to the higher acquisition bandwidth.

**References:** [1] Greenman, R.L, et al. Magn Reson Med, 2004, 52, p 1036-1042. [2] Greenman, R.L and Smithline, H.A. Acad Radiol, 2011, 18, p 917-923. [3] Magland, J. and Wehrl, F.W. Proc ISMRM 14<sup>th</sup> Scientific Meeting (2006). [4] Insko, E.K. and Bolinger, L. J Magn Reson Ser A, 1993, 103, p 82-85. [5] Bogner, W., et al. Magn Reson Med, 2009, 62, p 574-582. [6] Kholmovski, E.G., et al. J Magn Reson Imag, 2000, 11, p 549-558.

**Acknowledgments:** NIH R01-AR053133, R01-AR050260 and R01-AR060238

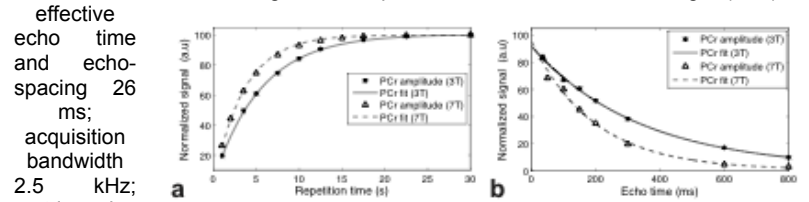


Fig. 2. **a**) T<sub>1</sub> measurement (calf muscle in healthy volunteer) at 3T (5.56 s) and 7T (3.49 s) **b**) T<sub>2</sub> measurement on the same volunteer at 3T (349 ms) and 7T (199 ms).

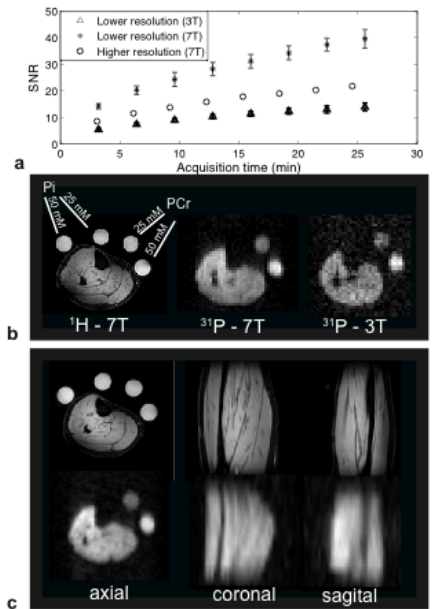


Fig. 3. **a**) SNR as a function of acquisition time at 3T and 7T. A 2.8 fold increase is observed. **b**) Comparison of an axial slice acquired in 25 min at 3T and 7T with the same (lower) resolution. **c**) Higher resolution image at 7T (acquired in 25 min) interpolated at the matrix size of the <sup>1</sup>H image.